

Multi-Lag Estimators for the Alternating Mode of Dual-Polarimetric Weather Radar Operation

David L. Pepyne
pepyne@ecs.umass.edu

Center for Collaborative Adaptive Sensing of the Atmosphere (CASA)
Dept. of Electrical and Computer Engineering
Univ. of Massachusetts, Amherst, MA 01003

1 Introduction

All National Weather Service (NWS) weather surveillance radars are and will continue to be dual-polarimetric [21], [19]. Dual-polarimetric weather radars measure the co-polar horizontally and vertically polarized returns from hydrometeors. This allows them to sense the size, shape, and state features of the hydrometeors, features the previous generation of single-pol (usually horizontally polarized) weather radars could not sense directly. The result is greatly improved quantitative precipitation estimation (QPE) and hydrometeor classification [6].

When processing weather radar data, multi-lag estimators allow for the estimation of signal powers (from which reflectivity and differential reflectivity are obtained) and co-polar cross-correlation coefficient (a measure of hydrometeor shape symmetry) without a need to first obtain estimates of the system noise powers [10], [11], [13]. Having such multi-lag estimators is useful since accurate noise power estimates can be difficult or time consuming to obtain [4], [9], [8].

Thus far, the only multi-lag estimators that have been developed have been for the simultaneous mode of polarimetric weather radar operation, where the horizontal and vertical polarizations are transmitted and received simultaneously by the radar. This makes sense, since virtually all operational polarimetric weather radars today are mechanically scanned parabolic dish radars, and these almost always operate in the simultaneous mode (e.g., the NWS, WSR-88DP, dual-pol NEXRAD).

Future plans are considering replacing the nation's aging mechanically scanned weather and aircraft surveillance radar systems with a network of multifunctional electronically scanned phased array radars that perform both tasks at the same time [18]. Because it simplifies

Presented at the American Meteorological Society's, 38th Conference on Radar Meteorology, Chicago, IL, August 29, 2017.

design complexity and reduces cost, these phased-array radars will likely operate in an alternating mode of polarimetric operation, where the radar alternates between the transmission and reception of horizontally and vertically polarized beams on consecutive pulses [1].

To accommodate these phased-array radar systems, this paper develops noise power independent multi-lag estimators for signal power, differential reflectivity, and co-polar cross-correlation coefficient for the alternating mode of polarimetric weather radar operation. The estimators are evaluated using simulated timeseries data and timeseries data from one of CASA’s X-band, polarimetric, phased-array radars shown in **Fig. 1** [15], [16].

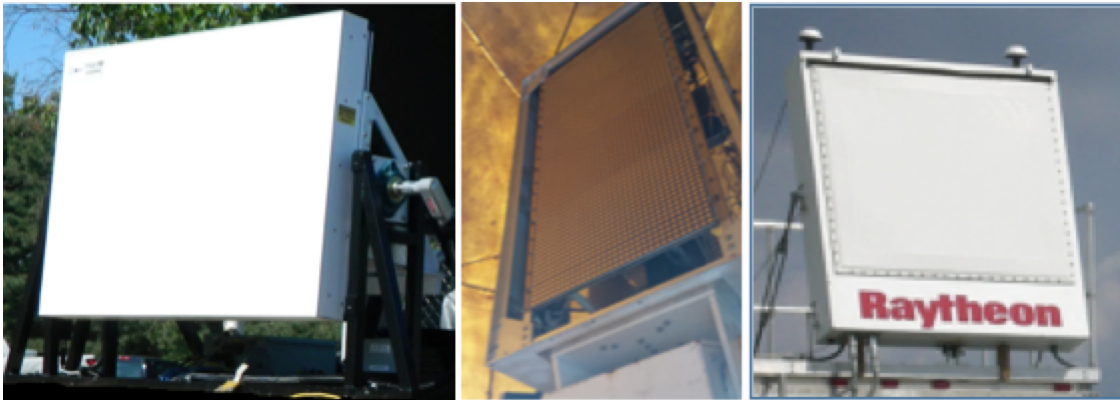


Figure 1: *CASA’s X-band, dual-polarimetric, phased-array radars. The phase-tilt (left) scans electronically in azimuth and mechanically in elevation. The phase-spin (center) scans mechanically in azimuth and electronically in elevation. The phase-phase (right), on loan from Raytheon Corp., scans electronically in both azimuth and elevation. Phased-arrays such as these are designed to operate alone or as part of a collaborating network [12].*

2 Background

As illustrated schematically in **Fig. 2**, *weather radars* probe the sky with a narrow pencil beam. Sampling in the receiver partitions the beam into *range bins*. The combination narrow beam and range bin partitioning allows weather radars to map the three dimensional structures of storms. *Polarimetric* weather radars use in effect two beams, one horizontally polarized (h-pol), another vertically polarized (v-pol). This enables the radar to measure the shape features of the hydrometeors, such as the flattening of raindrops as they fall through the beam.

2.1 Correlation Functions

Each range bin encloses a volume of atmosphere. The size of the volume is determined by the radar’s beamwidths, the spacing between consecutive range bins, and the range bin’s distance from the radar. For CASA’s phased-array radars with their two degree beamwidths

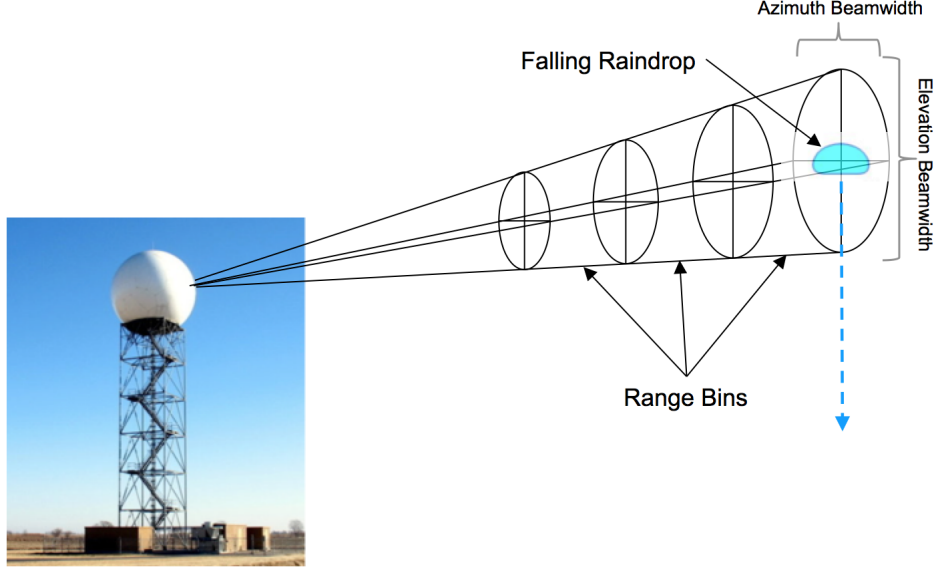


Figure 2: *Schematic of the beam from a dual-polarimetric weather radar.*

and 50 meter range bin spacings, range bin volumes vary from a few thousand cubic meters in size at the 1 km minimum range of the radar to a few million cubic meters in size at the 30-40 km maximum range of the radar. During precipitation, a range bin will therefore contain a huge number of individual hydrometers. The result is that the received co-polar h-pol and v-pol I,Q timeseries samples from a range bin are random processes whose auto- and cross-correlation functions are well modeled by Gaussians of the forms [5], [2], [10], [13]:^{1,2}.

$$R_{hh}(n) = S_h \exp \left[-\frac{8\pi^2 W^2 (nT_s)^2}{\lambda^2} \right] \exp \left[-j \frac{4\pi V n T_s}{\lambda} \right] + N_h \delta(n) \quad (1)$$

$$R_{vv}(n) = S_v \exp \left[-\frac{8\pi^2 W^2 (nT_s)^2}{\lambda^2} \right] \exp \left[-j \frac{4\pi V n T_s}{\lambda} \right] + N_v \delta(n) \quad (2)$$

$$R_{hv}(n) = \sqrt{S_h S_v} \rho_{hv} \exp \left[-\frac{8\pi^2 W^2 (nT_s)^2}{\lambda^2} \right] \exp \left[-j \frac{4\pi V n T_s}{\lambda} + j \phi_{dp} \right] \quad (3)$$

where $R_{hh}(n)$ ($R_{vv}(n)$) is the auto-correlation function associated with the I,Q stream resulting from the h-pol (v-pol) return to an h-pol (v-pol) transmitted pulse, and $R_{hv}(n)$ is the cross-correlation function relating h-pol and v-pol streams. In the equations:

- n is the lag index in number of pulses.

¹Co-polar returns are the horizontally (vertically) polarized returns from a horizontally (vertically) polarized pulse.

²Ground clutter is modeled as a very narrow Gaussian centered around zero Doppler. Here we assume that any ground clutter that may have been present in the I,Q timeseries has been removed, e.g., using ground clutter filtering techniques such as GMAP [17] or CLEAN-AP [20]

- T_s is the pulse repetition time (PRT) in seconds between pulses. $PRT = 1/PRF$, where PRF is the pulse repetition frequency in Hz. In this paper we assume constant PRT pulsing.
- λ is the radar’s wavelength. For CASA’s phased-array X-band radars, the wavelength is just over 3 cm.
- N_h and N_v represent the noise powers due predominately to thermal sources, internal and external to the radar. The $\delta(n)$ suggests that the noises uncorrelated in time. The noise power N_h is also assumed independent of the noise power N_v .

2.2 Weather Data Processing

The goal of weather data processing is to estimate the parameters of the correlation functions:

- S_h (S_v) represents the h-pol (v-pol) signal power scattered back to the radar from h-pol (v-pol) pulses. S_h is used to obtain the reflectivity, Z , which is a measure of hydrometeor concentration, and the ratio of the two powers is used to obtain the differential reflectivity, $Z_{dr} = 10\log_{10}(\frac{S_h}{S_v})$, which is a measure of hydrometeor shape symmetry. In rain, $S_h > S_v$, due to the flattening of raindrops as they fall, resulting in $Z_{dr} > 0$.
- V represents the mean radial velocity of the hydrometers in the range bin. $V < 0$ ($V > 0$) for hydrometers moving towards (away) from the radar.
- W represents the spectrum width giving the variation in radial velocity about the mean, e.g., due to turbulence and shear. Note that, in general, the spectrum width measured by a horizontally polarized beam can be slightly different from the spectrum width measured by a vertically polarized beam. These differences, due to wobble and spin, however, are generally so weak that they can be ignored.
- ρ_{hv} is the co-polar cross-correlation coefficient that measures the shape symmetry of the hydrometeors in the resolution volume. Taking values between 0 and 1, higher values of ρ_{hv} indicate greater similarity in the horizontal and vertical sizes of the hydrometeors in the range bin.
- ϕ_{dp} is the differential propagation phase whose rate of change with range (specific differential phase) measures, for example, the amount of liquid water in the path of the radar’s beam, the steeper the slope, the higher the rain rate.

2.3 Conventional “Noise Subtraction” Estimators

Estimators for the weather parameters can be obtained by mathematical manipulation of the correlations in equations (1)-(3) leading to the so-called autocovariance algorithms for

weather data processing [5], [2]. Conventional estimators for signal power, differential reflectivity, and correlation coefficient are based on “noise subtraction”:

$$S_h = |R_{hh}(0)| - N_h \quad (4)$$

$$S_v = |R_{vv}(0)| - N_v \quad (5)$$

leading to the differential reflectivity estimator,

$$\begin{aligned} Z_{dr} &= 10 \log_{10} \left(\frac{S_h}{S_v} \right) \\ &= 10 \log_{10} \left(\frac{|R_{hh}(0)| - N_h}{|R_{vv}(0)| - N_v} \right) \end{aligned} \quad (6)$$

and co-polar correlation coefficient estimator,

$$\begin{aligned} \rho_{hv} &= \frac{|R_{hv}(0)|}{\sqrt{S_h S_v}} \\ &= \frac{|R_{hv}(0)|}{\sqrt{(|R_{hh}(0)| - N_h)(|R_{vv}(0)| - N_v)}} \end{aligned} \quad (7)$$

Because the conventional estimators depend explicitly on the noise powers, they require some means to estimate them.

In general, the noise powers depend on internal and external, predominately, thermal sources. The implication is that the noise powers should ideally be estimated individually for each radial [8]. In a phased-array radar, the noise powers would also need to be re-estimated for any change in transceiver operating parameters, such as a change in receiver bandwidth resulting from an on-the-fly change in a pulse compressed waveform.

One approach for “radial based” noise power estimation would involve N “receive only” pulses generated with the transmitter turned off followed by M normal pulses generated with the transmitter turned on. The noise powers would be estimated from the receive only pulses, the weather parameters from the normal pulses. Receive only pulses are done by the Terminal Doppler Weather Radar (TDWR) – not at the start of each radial, but at the start of each azimuth sweep – for noise power estimation [3]. An alternative approach for radial based noise power estimation would involve generating pulses normally with the transmitter turned on, identifying and discarding range bins that contain signal, and estimating the noise powers from the signal free range bins that remain [4], [9], [8]. Such a method has been accepted for implementation in the WSR-88D [8].

Both of these approaches have issues when it comes to X-band phased-array radars. Receive only pulses would take away time from data collection, a particular problem for phased-array radars, which are intended to be multifunctional, interleaving weather surveillance with aircraft surveillance and tracking [19]. Estimating the noise from signal free range bins is a problem in that accurate noise estimation can require more signal free range bins than can be found in an X-band radar, which generally have short 30-40 km ranges, the entirety of which will often contain signal when weather is passing over the radar.

The various difficulties with accurate noise power estimation motivates the use of estimators that are independent of the noise powers. The papers [10], [11], [13] developed a number of multi-lag estimators, including estimators for signal power,

$$S_h = \frac{|R_{hh}(1)|^{4/3}}{|R_{hh}(2)|^{1/3}} \quad (8)$$

differential reflectivity,

$$Z_{dr} = 10 \log_{10} \left(\frac{|R_{hh}(1)|}{|R_{vv}(1)|} \right) \quad (9)$$

and correlation coefficient,

$$\rho_{hv} = \frac{0.5(|R_{hv}(-1)| + |R_{hv}(1)|)}{\sqrt{|R_{hh}(1)||R_{vv}(1)|}} \quad (10)$$

The advantage of these estimators is that because they do not use the lag-0 autocorrelations $R_{hh}(0)$ and $R_{vv}(0)$, they are independent of the noise powers. They thus avoid the need for noise power estimation.

3 Multi-Lag Extensions to the ALTERNATING Mode

The issue with the estimators developed in [10], [11], [13] is that they assume the SIMULTANEOUS or SHV mode of dual-polarimetric weather radar operation. Because the SHV mode requires transmitting and receiving both polarizations at the same time, it significantly complicates phased-array antenna design [1]. As a result, most dual-polarimetric phased-array radars, including all of CASA's, use the ALTERNATING or AHV mode in which the radar transmits and receives only one polarization at a time, alternating between the two polarizations on consecutive pulses. **Fig. 3** compares the two modes.

The SHV mode leads to the correlations in equations (1)-(3), where, because both polarizations are received with each pulse, the correlations are defined for all lags. Since the AHV mode only receives one polarization at a time, the correlations are not defined for all lags. In particular, the cross-correlation is not defined for lag-0. The AHV mode thus leads to a different set of correlation functions, requiring a different set of estimators.

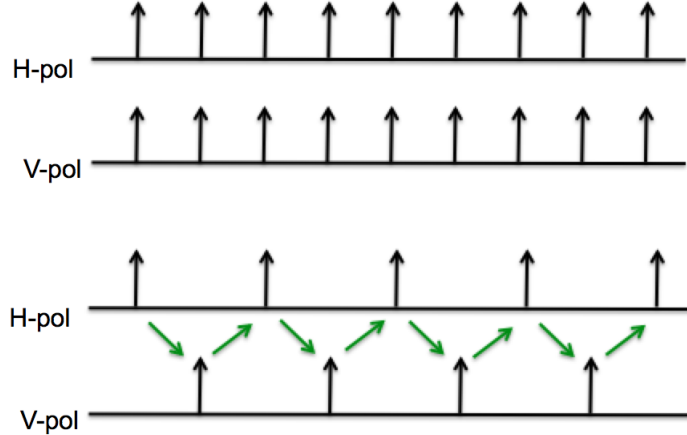


Figure 3: *Schematic comparing the SHV mode of dual-polarimetric weather radar operation (top) to the AHV mode (bottom). The SHV mode transmits and receives both polarizations with each pulse. The AHV mode transmits and receives one polarization at a time, alternating between polarizations on consecutive pulses.*

To relate the AHV mode to the SHV, let x be the stream of co-polar AHV h-pol I,Q samples and y the stream of co-polar AHV v-pol I,Q samples. Noting that the AHV h- and v-pol samples come at half the rate as their corresponding SHV samples and that the AHV h- and v-pol samples are produced with a lag of two pulses between consecutive h-pol (v-pol) samples, we have,

$$R_{xx}(n) = R_{hh}(2n) \quad (11)$$

$$R_{yy}(n) = R_{vv}(2n) \quad (12)$$

$$R_{xy}(n) = R_{hv}(2n - 1) \quad (13)$$

where $R_{xx}(n)$ and $R_{yy}(n)$ are the x, y autocorrelation functions respectively and $R_{xy}(n)$ is the cross-correlation function between the x and y I/Q streams.

3.1 Conventional AHV Estimators

Conventional AHV estimators for signal power have the same “noise subtraction” form as in the SHV case,

$$S_h = |R_{xx}(0)| - N_h \quad (14)$$

and

$$S_v = |R_{yy}(0)| - N_v \quad (15)$$

As a result, the AHV differential reflectivity estimator has the same form as the SHV estimator,

$$Z_{dr} = 10 \log_{10} \left(\frac{S_h}{S_v} \right) \quad (16)$$

On the other hand, because it is not possible to obtain $R_{hv}(0)$ from $R_{xy}(n)$ (see equation (13)), the AHV estimator for cross-correlation has a much different form than the SHV estimator. There are a number of AHV estimators for correlation coefficient, cf. [5], [2]. The estimator we use in the performance section of this paper is the recent one from [14],

$$\rho_{hv} = \frac{0.5(|R_{xy}(0)| + |R_{xy}(1)|)}{(S_h S_v)^{3/8} |R_{xx}(1) R_{yy}(1)|^{1/8}} \quad (17)$$

Again, because the signal powers that appear in the conventional AHV estimators depend explicitly on the noise powers, their implementation would require some means for noise power estimation.

3.2 Multi-Lag AHV Estimators

Using equations (1)-(3) along with the relationships in equations (11)-(13) in this section we extend the multi-lag estimator concept to the AHV mode by deriving AHV multi-lag estimators for signal power, differential reflectivity, and correlation coefficient. Similar to their SHV counterparts, the advantage of the estimators we develop is that they are independent of the noise powers.

3.2.1 Signal Power

A multi-lag estimator for signal power for the AHV mode follows immediately from the multi-lag estimator for the SHV mode,

$$\begin{aligned}
\frac{|R_{xx}(1)|^{4/3}}{|R_{xx}(2)|^{1/3}} &= \frac{|R_{hh}(2)|^{4/3}}{|R_{hh}(4)|^{1/3}} \\
&= \frac{|S_h \exp\left[-\frac{8\pi^2 W^2 (2T_s)^2}{\lambda^2}\right] \exp\left[-j\frac{4\pi V 2T_s}{\lambda}\right] + N_h \delta(2)|^{4/3}}{|S_h \exp\left[-\frac{8\pi^2 W^2 (4T_s)^2}{\lambda^2}\right] \exp\left[-j\frac{4\pi V 4T_s}{\lambda}\right] + N_h \delta(4)|^{1/3}} \\
&= \frac{\left(S_h \times \exp\left[-\frac{8\pi^2 W^2 T_s^2}{\lambda^2}\right]^4 \times 1 + 0\right)^{4/3}}{\left(S_h \times \exp\left[-\frac{8\pi^2 W^2 T_s^2}{\lambda^2}\right]^{16} \times 1 + 0\right)^{1/3}} \\
&= \frac{S_h^{4/3} \exp\left[-\frac{8\pi^2 W^2 T_s^2}{\lambda^2}\right]^{4(4/3)}}{S_h^{1/3} \exp\left[-\frac{8\pi^2 W^2 T_s^2}{\lambda^2}\right]^{16(1/3)}} \\
&= S_h
\end{aligned}$$

resulting in,

$$S_h = \frac{|R_{xx}(1)|^{4/3}}{|R_{xx}(2)|^{1/3}} \quad (18)$$

3.2.2 Differential Reflectivity

A multi-lag estimator for differential reflectivity for the AVH mode follows immediately from the multi-lag estimator for the SHV mode,

$$\begin{aligned}
10\log_{10}\left(\frac{|R_{xx}(1)|}{|R_{yy}(1)|}\right) &= 10\log_{10}\left(\frac{|R_{hh}(2)|}{|R_{vv}(2)|}\right) \\
&= 10\log_{10}\left(\frac{S_h \times \exp\left[-\frac{8\pi^2 W^2 T_s^2}{\lambda^2}\right]^4 \times 1 + 0}{S_v \times \exp\left[-\frac{8\pi^2 W^2 T_s^2}{\lambda^2}\right]^4 \times 1 + 0}\right) \\
&= 10\log_{10}\left(\frac{S_h}{S_v}\right) \\
&= Z_{dr}
\end{aligned}$$

resulting in,

$$Z_{dr} = 10\log_{10}\left(\frac{|R_{xx}(1)|}{|R_{yy}(1)|}\right) \quad (19)$$

3.2.3 Correlation Coefficient

Like the other estimators, our multi-lag estimator for correlation coefficient for the AHV mode starts with the multi-lag estimator for the SHV mode,

$$\rho_{hv} = \frac{0.5(|R_{hv}(-1)| + |R_{hv}(1)|)}{\sqrt{|R_{hh}(1)||R_{vv}(1)|}} \quad (20)$$

Regarding the numerator, we can use the relationship,

$$R_{xy}(n) = R_{hv}(2n - 1) \quad (21)$$

to obtain,

$$0.5(|R_{hv}(-1)| + |R_{hv}(1)|) = 0.5(|R_{xy}(0)| + |R_{xy}(1)|) \quad (22)$$

Regarding the terms in the denominator, however, we have the issue that since $R_{xx}(n) = R_{hh}(2n)$ and $R_{yy}(n) = R_{vv}(2n)$, we cannot estimate $|R_{hh}(1)|$ and $|R_{vv}(1)|$ directly and must estimate them indirectly. To do so, consider the magnitude curve $|R_{hh}(n)|, n = \dots -1, 0, 1 \dots$ in **Fig. 4**. Without noise, the curve has the form of a Gaussian. That is, when $N_h = 0$, the

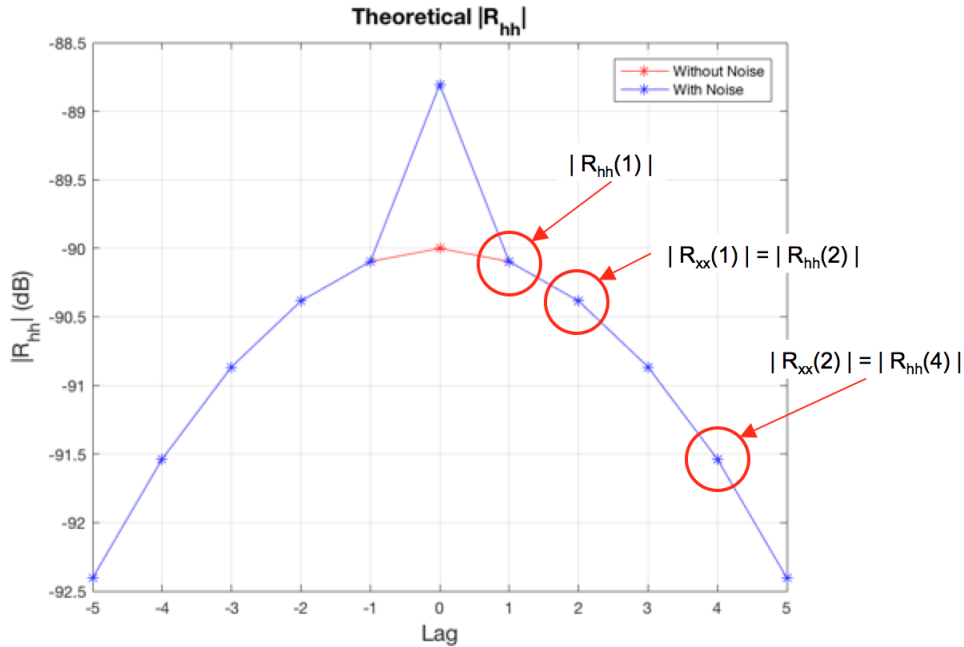


Figure 4: *Theoretical magnitude curve $|R_{hh}(n)|$. Without noise (red), the curve is Gaussian. The goal is to obtain an approximation for $|R_{hh}(1)|$ using the AHV correlation magnitudes $|R_{xx}(1)|$ and $|R_{xx}(2)|$.*

auto-correlation magnitude curve can be written as,

$$\begin{aligned}
|R_{hh}(n)| &= |S_h \exp \left[-\frac{8\pi^2 W^2 (nT_s)^2}{\lambda^2} \right] \exp \left[-j \frac{4\pi V n T_s}{\lambda} \right]| \\
&= S_h \times \exp \left[-\frac{8\pi^2 W^2 (nT_s)^2}{\lambda^2} \right] \\
&= S_h \times \exp \left[-\frac{8\pi^2 W^2 T_s^2 n^2}{\lambda^2} \right] \\
&= a \times \exp \left[-\frac{n^2}{2c^2} \right]
\end{aligned} \tag{23}$$

with the parameters a and c defining the height and width of the Gaussian curve. If we can obtain estimates for a and c , then we have the approximation,

$$|R_{hh}(1)| = a \times \exp \left[-\frac{1}{2c^2} \right] \tag{24}$$

To obtain estimates for the parameters a and c , we will use the observed correlations $|R_{xx}(1)| = |R_{hh}(2)|$ and $|R_{xx}(2)| = |R_{hh}(4)|$, see **Fig. 4**. With these observed correlations, we get two equations for the two unknowns,

$$\begin{aligned}
|R_{xx}(1)| &= a \times \exp \left[-\frac{(n=2)^2}{2c^2} \right] \\
&= a \times \exp \left[-\frac{4}{2c^2} \right] \\
&= a \times \exp \left[-\frac{2}{c^2} \right]
\end{aligned} \tag{25}$$

and

$$\begin{aligned}
|R_{xx}(2)| &= a \times \exp \left[-\frac{(n=4)^2}{2c^2} \right] \\
&= a \times \exp \left[-\frac{16}{2c^2} \right] \\
&= a \times \exp \left[-\frac{8}{c^2} \right]
\end{aligned} \tag{26}$$

Solving the first equation for a we obtain,

$$a = |R_{xx}(1)| \exp \left[+\frac{2}{c^2} \right] \quad (27)$$

Plugging this into the second equation and solving for c , we obtain,

$$\begin{aligned}
|R_{xx}(2)| &= a \times \exp \left[-\frac{8}{c^2} \right] \\
&= |R_{xx}(1)| \exp \left[+\frac{2}{c^2} \right] \exp \left[-\frac{8}{c^2} \right] \\
&= |R_{xx}(1)| \exp \left[+\frac{2}{c^2} - \frac{8}{c^2} \right] \\
&= |R_{xx}(1)| \exp \left[+\frac{-6}{c^2} \right] \\
\Rightarrow \ln \left(\frac{|R_{xx}(2)|}{|R_{xx}(1)|} \right) &= \frac{-6}{c^2} \\
\Rightarrow c^2 &= \frac{-6}{\ln \left(\frac{|R_{xx}(2)|}{|R_{xx}(1)|} \right)} \\
\Rightarrow c &= \sqrt{\frac{-6}{\ln \left(\frac{|R_{xx}(2)|}{|R_{xx}(1)|} \right)}} \quad (28)
\end{aligned}$$

Plugging the results into (24) and solving we get the approximation,

$$\begin{aligned}
|R_{hh}(1)| &= a \times \exp \left[-\frac{1}{2c^2} \right] \\
&= |R_{xx}(1)| \exp \left[\frac{2}{c^2} \right] \exp \left[\frac{-1}{2c^2} \right] \\
&= |R_{xx}(1)| \exp \left[\frac{3}{2} \frac{1}{c^2} \right] \\
&= |R_{xx}(1)| \exp \left[\frac{3}{2} \frac{1}{\frac{-6}{\ln\left(\frac{|R_{xx}(2)|}{|R_{xx}(1)|}\right)}} \right] \\
&= |R_{xx}(1)| \exp \left[-\frac{3}{12} \ln\left(\frac{|R_{xx}(2)|}{|R_{xx}(1)|}\right) \right] \\
&= |R_{xx}(1)| \exp \left[-\frac{1}{4} \ln\left(\frac{|R_{xx}(2)|}{|R_{xx}(1)|}\right) \right] \\
&= |R_{xx}(1)| \exp \left[\ln\left(\frac{|R_{xx}(2)|}{|R_{xx}(1)|}\right) \right]^{-1/4} \\
&= |R_{xx}(1)| \left[\frac{|R_{xx}(2)|}{|R_{xx}(1)|} \right]^{-1/4} \\
&= |R_{xx}(1)|^{5/4} |R_{xx}(2)|^{-1/4}
\end{aligned} \tag{29}$$

A similar derivation gives us an approximation for $|R_{vv}(1)|$,

$$|R_{vv}(1)| = |R_{yy}(1)|^{5/4} |R_{yy}(2)|^{-1/4} \tag{30}$$

Plugging the approximations in (29) and (30) into equation (20) and simplifying we obtain a multi-lag estimator for correlation coefficient for the AHV mode,

$$\begin{aligned}
\rho_{hv} &= \frac{0.5(|R_{hv}(-1)| + |R_{hv}(1)|)}{\sqrt{|R_{hh}(1)||R_{vv}(1)|}} \\
&= \frac{0.5(|R_{xy}(0)| + |R_{xy}(1)|)}{\sqrt{|R_{xx}(1)|^{5/4} |R_{xx}(2)|^{-1/4} |R_{yy}(1)|^{5/4} |R_{yy}(2)|^{-1/4}}} \\
&= \frac{0.5(|R_{xy}(0)| + |R_{xy}(1)|)}{|R_{xx}(1)|^{5/8} |R_{xx}(2)|^{-1/8} |R_{yy}(1)|^{5/8} |R_{yy}(2)|^{-1/8}} \\
&= \frac{0.5(|R_{xy}(0)| + |R_{xy}(1)|) |R_{xx}(2)|^{1/8} |R_{yy}(2)|^{1/8}}{|R_{xx}(1)|^{5/8} |R_{yy}(1)|^{5/8}}
\end{aligned} \tag{31}$$

1. Generate two independent white noise processes, each consisting of M samples;
2. Correlate them according to ρ_{hv} ;
3. “Color” them via filtering to give them Gaussian spectra with parameters, T_s , λ , V and W ;
4. Scale them to give them the signal powers S_h and S_v (equivalently to give them a desired SNR and Z_{dr} , in which case, $S_h = N_h \times 10^{SNR/10}$ and $S_v = \frac{S_h}{10^{Z_{dr}/10}}$);
5. Shift the phase between the two processes to according to ϕ_{dp} ;
6. Add to each process an independent white noise process, one with power N_h , the other with power N_v ;
7. Extract the M AHV I,Q samples from the resulting SHV samples.

Table 1: *Pseudocode for an I,Q weather data simulator.*

4 Performance Results

This section compares the multi-lag estimators for the AHV mode in equations (18), (19), (31) to the conventional estimators for the AHV mode in equations (14), (16), (17). This is done first using simulated I,Q timeseries and then using actual I,Q timeseries from one of CASA’s X-band, polarimetric, AHV radars.

4.1 Simulation Results

The correlation functions in equations (1)-(3) tell us how to simulate I,Q timeseries from a clutter free range bin uniformly filled with (assumed liquid) hydrometeors. Pseudocode is listed in **Table 1**, see also [7]. As we see from the table, the inputs to the I,Q simulator are the desired weather parameters S_h , S_v , V , W , ρ_{hv} , and ϕ_{dp} , the assumed radar wavelength λ and noise powers N_h and N_v , and the assumed radar operating parameters T_s and number of samples per radial M . The output is M AHV I,Q samples whose correlations satisfy the input parameters.

Similar to the evaluations of the SHV multi-lag estimators in [10], [11], we use the I,Q simulator to evaluate the AHV estimator performances in terms of their error biases and standard deviations as functions of spectrum width. The performance estimates are obtained by performing 1000 Monte Carlo experiments, each using a new set of randomly generated I,Q samples. The simulation parameters used to generate the I,Q samples are listed in **Table 2**. The results are shown in **Figs. 5-7**. In generating the results we assume that when we do the noise subtraction for the conventional estimators we know the noise powers N_h and N_v exactly. As seen in **Figs. 5-7**, except for the standard deviation of correlation coefficient, the performances of the multi-lag AHV estimators are nearly identical to the performances of the conventional AHV estimators.

The SENSR document [19] gives the performances that will need to be met by any future WSR-88D replacement. It is of interest, therefore, to see how the AHV estimators perform

Variable	Value	Units	Remarks
SNR	5	dB	
Z_{dr}	1	dB	
ρ_{hv}	0.97		
V	2	m/s	The velocity value is arbitrary since the results depend only on correlation magnitudes.
ϕ_{dp}	10	deg	The differential phase value is arbitrarily since the results depend only on correlation magnitudes.
λ	0.0318	m	This corresponds to the X-band radar center frequency of 9.41 GHz. All of CASA's phased-array radars operate in the X-band.
N_h, N_v	-95, -95	dBW	These are typical noise power values for CASA's phased-array radars.
M	128	pulses/radial	
T_s	266.7	μs	This corresponds to a $PRF = 3750$ Hz. This is the maximum PRF for an unambiguous range of 40 km. It leads to an AHV x (or y) data unambiguous velocity of 14.9 m/s.

Table 2: Parameters used for the simulation of the I, Q timeseries samples used in the evaluation of the AHV estimators.

against the SENSR requirements. SENSR does not give an explicit requirement for signal power, but it does give explicit requirements for differential reflectivity and correlation coefficient. These are listed in **Table 3**.

Variable	SNR	W	ρ_{hv}	Bias	Standard Deviation
Z_{dr}	20dB	2m/s	0.99	≤ 0.2 dB	≤ 0.4 dB
ρ_{hv}	10dB	4m/s	0.99	≤ 0.006	
ρ_{hv}	20dB	2m/s	0.99		≤ 0.006

Table 3: SENSR requirement for correlation coefficient.

Running the I,Q simulator with the SENSR parameters (i.e., SNR , W , and ρ_{hv} as in **Table 3**, the remaining parameters as in **Table 2**) we get the AHV estimator performances in **Table 4**. As seen, for $M = 128, PRF = 3750$, both the conventional and multi-lag AHV estimators meet the differential reflectivity requirements. For $M = 128, PRF = 3750$, the conventional AHV estimator also meets the requirements on correlation coefficient. The multi-lag estimator, on the other hand, can only meet the correlation coefficient requirements if the number of pulses and/or PRF is increased. This is illustrated in **Table 5**, where the number of pulses has been increased to $M = 150$ and the pulse rate to $PRF = 4250$ Hz.

Variable		Bias	Standard Deviation
Z_{dr}	Requirement	0.2 dB	0.4 dB
	Conventional	0.0076 dB	0.2606 dB
	Multi-Lag	0.0081 dB	0.2729 dB
ρ_{hv}	Requirement	0.006	0.006
	Conventional	0.0021	0.0054
	Multi-Lag	0.0106	0.0062

Table 4: *AHV estimator performances relative to the SENSR requirements for $M = 128$ and $PRF = 3750$ Hz (giving maximum unambiguous range = 40 km and maximum unambiguous velocity = 14.9 m/s).*

Variable		Bias	Standard Deviation
ρ_{hv}	Requirement	0.006	0.006
	Conventional	0.0014	0.0053
	Multi-Lag	0.0023	0.0054

Table 5: *AHV estimator performances relative to the SENSR correlation coefficient requirement for $M = 150$ and $PRF = 4250$ Hz (giving maximum unambiguous range = 35 km and maximum unambiguous velocity = 16.9 m/s).*

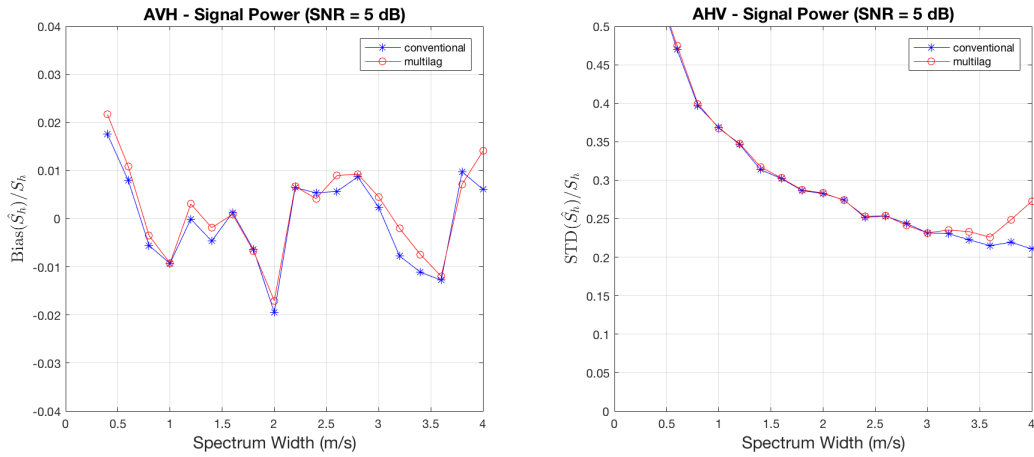


Figure 5: *Simulated estimator performances for signal power S_h for the simulation parameters in Table 2.*

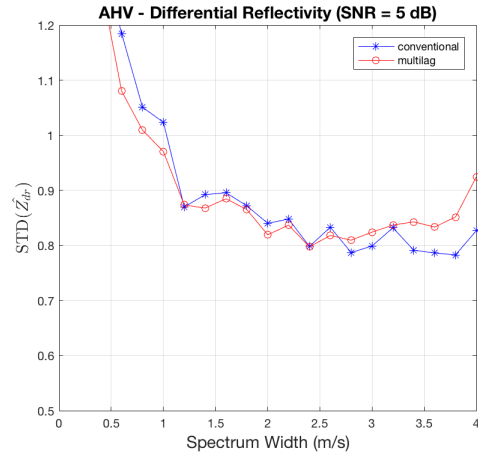
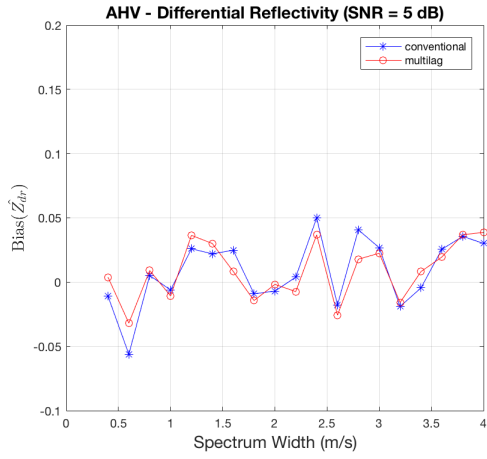


Figure 6: Simulated estimator performances for differential reflectivity Z_{dr} for the simulation parameters in **Table 2**.

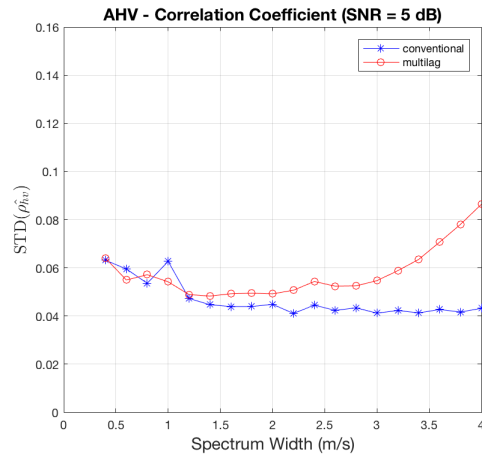
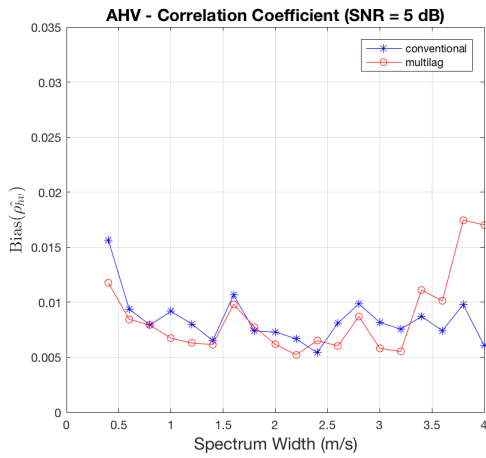


Figure 7: Simulated estimator performances for correlation coefficient ρ_{nv} for the simulation parameters in **Table 2**.

4.2 Real Data Results

In addition to the simulation experiments, we also compared the multi-lag and conventional estimators for correlation coefficient using I,Q data from one of CASA's X-band, polarimetric, AHV, phased-array radars. The radar's range was set to 30 km, 64 pulses were used per radial, and the PRF was set at 3900 Hz. The radar uses pulse compressed waveforms, a short pulse for the first 10 km, a long pulse for the remaining 20 km.

Fig. 8 compares range profiles of SNR, spectrum width, and correlation coefficient. In the figure, the conventional correlation coefficient estimate is in blue and the multi-lag estimate is in red. As seen, the match between the conventional and multi-lag estimator is reasonably good, except where the signal-to-noise ratio (SNR) is low or the spectrum width (W) gets large, which we expect given the simulation results in **Fig. 7**. The close match in the performance of the conventional and multi-lag estimators is shown again in the PPI (plan position indication) plots in **Fig. 9**.

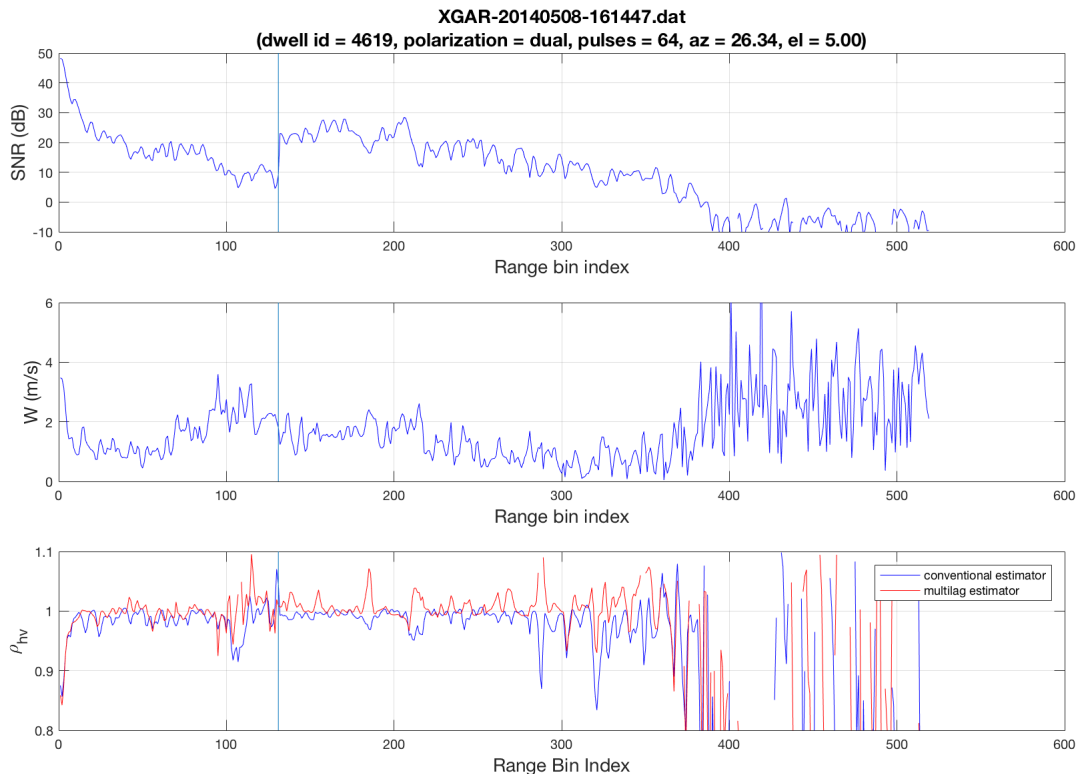


Figure 8: Range profile from one of CASA's phased-array radars comparing the conventional correlation coefficient estimator (ρ_{hv}) to the multi-lag estimator as functions of signal-to-noise ratio (SNR) and spectrum width (W).

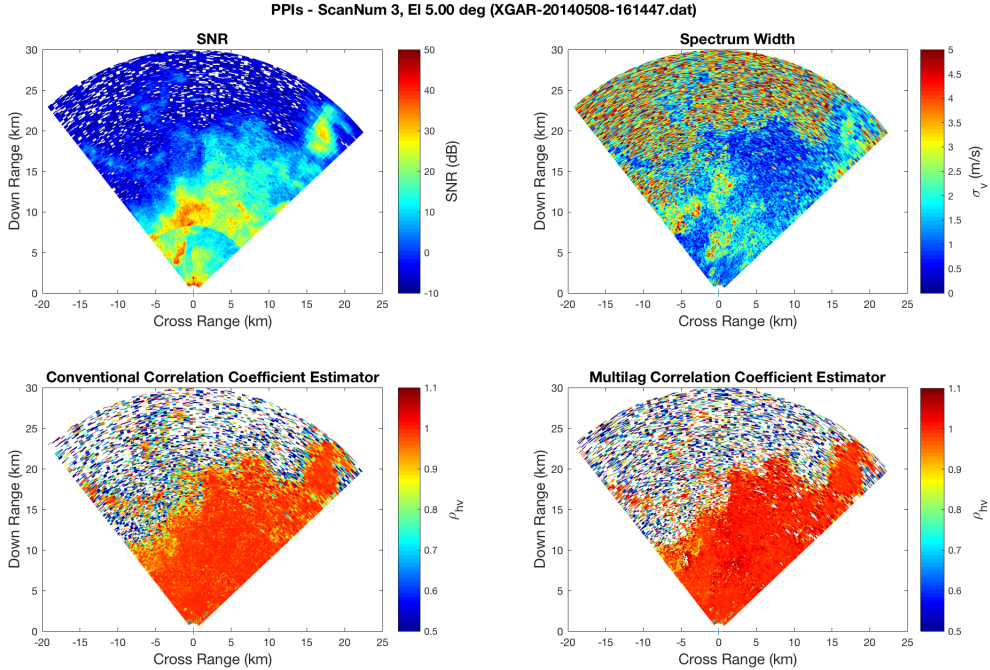


Figure 9: *Plan Position Indication (PPI) scan from one of CASA’s phased-array radars comparing the conventional correlation coefficient estimator (ρ_{hv}) to the multi-lag estimator as functions of signal-to-noise ratio (SNR) and spectrum width (W).*

5 Summary and Conclusions

Conventional estimators of signal power, differential reflectivity, and co-polar correlation coefficient in dual-pol weather radars require estimates of the system noise powers. Since the noise powers are due to both internal and external factors, estimates should ideally be done for each radial. For the next-generation multi-functional, short-range phased-array radars being developed, noise power estimators can take away precious time from data collection or may not give results during the critical times when weather is passing over the radar.

To avoid the need for noise power estimation, prior literature developed so-called “multi-lag” estimators for the SHV mode of dual-pol weather radar operation where the I,Q time-series from both polarizations is simultaneously available with each pulse. These estimators, because they do not use the lag-0 autocorrelations are independent of the system noise powers. In this paper we extended the multi-lag estimator concept to the AHV mode, which, due to design complexity, may be the most cost effective choice for the future polarimetric phased-arrays.

Simulation results and comparisons on actual data from one of CASA’s X-band, dual-polarimetric, AHV, phased-array radar showed the new AHV multi-lag estimators compare favorably to their conventional counterparts, even in the unrealistic case where the conventional estimators were given exact, error free value of the noises.

References

- [1] S.M. Bachmann, M. Tracy, and Y. Al-Rashid, "Mode of Dual Polarization: Phased Array Versus Parabolic Dish," *Proc. of the 34th AMS Conf. on Radar Meteorology*, 5-9 October, 2009.
- [2] V.N. Bringi and V. Chandrasekar, *Polarimetric Doppler Weather Radar: Principles and Applications*, Cambridge, 2001
- [3] J.Y.N. Cho, *Signal Processing Algorithms for the Terminal Doppler Weather Radar: Build 2*, Project Report, ATC-363, MIT Lincoln Labs, February 21, 2010.
- [4] M. Dixon and J.C. Hubbert, "The Separation of Noise and Signal Components in Doppler RADAR Returns," *7th European Conf. on Radar in Meteorology and Hydrology (ERAD 2012)*, 2012.
- [5] R.J. Doviak and D.S. Zrnica, *Doppler Radar and Weather Observations*, Dover, 1993
- [6] *Dual-Polarization Radar Training for NWS Partners*, NWS Warning Decision Training Branch. On-line courses at:
<http://training.weather.gov/wdtd/courses/dualpol/Outreach/>
- [7] G. Galati and G. Pavan, "Computer Simulation of Weather Radar Signals," *Simulation Practice and Theory*, Vol. 3, No. 1, pp. 17-44, July 1995.
- [8] I.R. Ivic, C. Curtis, and S.M. Torres, "Radial-Based Noise Power Estimation for Weather Radars," *Journal of Atmospheric and Oceanic Technology*, Vol. 30, December 2013.
- [9] I.R. Ivic and S.M. Torres, "Online Determination of Noise Level in Weather Radars," *6th European Conference on Radar in Meteorology and Hydrology (ERAD 2010)*, 2010.
- [10] L. Lei, G. Zhang, R. Palmer, B.-L. Cheong, M. Xue, and Q. Cao, "A Multi-Lag Correlation Estimator for Polarimetric Radar Variables in the Presence of Noise," *Proc. of the 34th AMS Conf. on Radar Meteorology*, 2009.
- [11] L. Lei, G. Zhang, R.J. Doviak, R. Palmer, B.-L. Cheong, M. Xue, Q. Cao, and Y. Li, "Multilag Correlation Estimators for Polarimetric Radar Measurements in the Presence of Noise," *Journal of Atmospheric and Oceanic Technology*, Vol. 29, pp. 772-795, June 2012.
- [12] D.J. McLaughlin, D.L. Petyne, V. Chandrasekar, et al., "Short Wavelength Technology and the Potential for Distributed Networks of Small Radar Systems," *Bulletin of the American Meteorological Society*, Vol. 90, No. 12, December 2009.
- [13] V.M. Melnikov and D.S. Zrnica, "Autocorrelation and Cross-Correlation Estimators of Polarimetric Variables," *Journal of Atmospheric and Oceanic Technology*, August, 2007.
- [14] V.M. Melnikov and D.S. Zrnica, "On the Alternate Transmission Mode for Polarimetric Phased Array Weather Radar," *Journal of Atmospheric and Oceanic Technology*, Vol. 32, February 2015

- [15] K. Orzel, *X-band Dual Polarization Phased-Array Radar for Meteorological Applications*, Ph.D. Dissertation, Dept. of Electrical and Computer Engineering, Univ. of Massachusetts, Amherst, February 2015.
- [16] R.A. Palumbo, *Applications in Low-Power Phased Array Weather Radars*, Ph.D. Dissertation, Dept. of Electrical and Computer Engineering, Univ. of Massachusetts, Amherst, February 2016.
- [17] A.D. Siggia and R. E. Passarelli, “Gaussian model adaptive processing (GMAP) for improved ground clutter cancellation and moment calculation,” *Third European Conference on Radar in Meteorology and Hydrology (ERAD)*, 2004.
- [18] *Spectrum Efficient National Surveillance Radar (SENSR): Concept of Operations*, Version 0.9, October 7, 2016. Available on-line at:
<https://www.fbo.gov/>
- [19] *Spectrum Efficient National Surveillance Radar (SENSR): Preliminary Performance Requirements*, Version 0.9, October 7, 2016. Available on-line at:
<https://www.fbo.gov/>
- [20] D.A. Warde and S.M. Torres, “Automatic Detection and Removal of Ground Clutter Contamination on Weather Radar,” *34th AMS Conf. on Radar Meteorology*, Williamsburg, VA, October 2009.
- [21] *WSR-88D Dual Polarization Deployment Progress*, June 24, 2013. Available on-line at:
<https://www.roc.noaa.gov/WSR88D/PublicDocs/DualPol/DPstatus.pdf>